Mutagenesis, 2015, 30, 59–66
doi:10.1093/mutage/geu057
Original Article

OXFORD

Original Manuscript

Effect of silver nanoparticles on mitogen-activated protein kinases activation: role of reactive oxygen species and implication in DNA damage

Alessandra Rinna[1,2,*], Zuzana Magdolenova[1], Alexandra Hudecova[1], Marcin Kruszewski[3,4], Magne Refsnes[5] and Maria Dusinska[1]

[1]Health Effects Laboratory, Environmental Chemistry Department, NILU-Norwegian Institute for Air Research, PO Box 100, 2027 Kjeller, Norway, [2]Department of Biomaterials, Institute of Clinical Dentistry, University of Oslo, PO Box 1109 Blindern, 0317 Oslo, Norway, [3]Centre for Radiobiology and Biological Dosimetry, Institute of Nuclear Chemistry and Technology, Dorodna 16, 03-195 Warszawa, Poland, [4]Institute of Rural Health, Jaczewskiego 2, 20-090 Lublin, Poland and [5]Department of Air Pollution and Noise, Norwegian Institute of Public Health, PO Box 4404 Nydalen, 0403 Oslo, Norway

*To whom correspondence should be addressed. Department of Biomaterials, Institute of Clinical Dentistry, University of Oslo, PO Box 1109, Blindern 0317, Oslo, Norway. Tel: +47 22852353; Fax: +47 22852053; Email: alessandra.rinna@odont.uio.no

Received June 19 2014; Revised September 17 2014; Accpeted September 17 2014.

Abstract

Large quantities of engineered nanoparticles (NP), such as nanosilver (AgNP), have been widely applied, leading to an increased exposure and potential health concerns. Herein, we have examined the ability of AgNP to induce reactive oxygen species (ROS), their role in genotoxic effects and the involvement of mitogen-activated protein kinases (MAPK). AgNP exposure induced ROS production in human epithelial embryonic cells which could be decreased by diphenyleneiodonium (DPI), an inhibitor of NADPH oxidases. Extracellular signal-regulated kinase (ERK) and c-Jun N-terminal kinase (JNK) phosphorylation, induced by AgNP, was an early response but not sustained in time. Furthermore, JNK and ERK activation could be inhibited by both DPI and a free radicals scavenger *N*-acetyl cysteine. We also investigated the role of MAPK in the DNA damage. Using a modified comet assay for the specific detection of hOGG1 sensitive sites, we showed that AgNP induced DNA oxidation after 30-min treatment, whereas no response was observed after 2 h. In conclusion, AgNP seem to induce DNA damage via a mechanism involving ROS formation. The oxidative DNA damage observed was transient, likely due to DNA repair; furthermore, higher damage was achieved upon inhibition of ERK activation by pre-treatment with U0126, suggesting a role for ERK in DNA damage repair. Activation of different MAPK might play an important role in the NP toxicity outcomes; understanding this process may be helpful for the identification of NP toxicity.

Introduction

Due to their size, engineered nanoparticles (NP) differ from the corresponding bulk material; their unique physicochemical properties are impressive from a material science perspective but may otherwise be undesirable because of more aggressive forms of toxicity (1). Chemical composition and catalytic activity of NP may enhance toxicity through the ability to react repeatedly with DNA, proteins and membranes and their long-term persistence in the host cell (2). The interaction between NP and macromolecules could have many consequences such as membrane permeability changes, signalling effects, enzyme inhibition, oxidant injuries and mutational alteration.

Despite major efforts to understand the adverse effects of NP, there is still a serious lack of information concerning the potential hazardous effects of manufactured NP on human health.

Based on the data that Woodrow Wilson Center's Project on Emerging Nanotechnologies (PEN) has collected, nanosilver (AgNP) appears to be the most common nanomaterial used today in manufactured consumer products (PEN, 2009, 196774). More than 25% of the products included in the PEN inventory, including cosmetics,

fabrics, toothpaste, toothbrushes, kitchen surfaces, plasters and medical equipment, are listed as containing AgNP. As the widespread exploitation of AgNP mainly arises from their antimicrobial properties, it is necessary to consider and determine if toxicity is mediated by AgNP within mammalian cells. It has, however, been shown in different mammalian models that AgNP may enter the body via different exposure routes and translocate to various organs where they can exert toxic effects depending on the dose applied. The potential to exert cytotoxic effects as observed by increased necrosis and apoptosis, and decreased proliferation, has also been revealed upon *in vitro* exposure, with the extent of cytotoxicity depending on size, intracellular release of silver ions, agglomeration and functionalisation of the AgNP, the concentrations and cell types used (3, 4). Although conflicting results have been found (5), AgNP have been also shown to cause genotoxic effects, such as DNA strand breaks, point mutations and DNA base oxidation (6–10).

Reactive oxygen species (ROS) generation and oxidative stress have been proposed to be likely mechanisms by which AgNP induce toxicity (11). Under normal conditions, ROS are generated, at low frequency, during cell respiration in the mitochondrial electron transport chain, but they are easily neutralised by antioxidant defences. However, under condition of stress such as during NP exposure, an excess of ROS production can occur and the antioxidant defences available may be overwhelmed resulting in a fall in glutathione reduced/glutathione oxidized (GSH/GSSG) ratio. The excess of ROS production might be due to enzymatic or non-enzymatic mechanisms. It has been shown that NP can interact and interfere with the function of proteins. An example is the NADPH oxidase (NOX) family, which is directly responsible for the production of superoxide radicals in the cells. In a study on pulmonary endothelium, NOX was reported to be involved in ROS generation following exposure to ultrafine particles (12).

It has been proposed that ROS play a role in AgNP genotoxicity but information about the downstream pathways through which AgNP signal in human cells and induce DNA damage is still very limited (9, 13, 14).

Mitogen-activated protein kinases (MAPK) are a group of serine-threonine proteins responsible for modulating many cellular responses. This group includes extracellular signal-regulated kinase (ERK), p38MAPK and c-Jun N-terminal kinase (JNK). To date, only few studies have been reported on the activation of MAPK signal pathways by AgNP resulting in a lack of information regarding the mechanisms underlying AgNP toxicity (15).

The aim of the current study was to provide an insight into the mechanisms of AgNP toxicity. We investigated the possible sources of ROS production as a major contributor to oxidative stress induced by AgNP. Further, we studied the activation of JNK and ERK and whether it is mediated by a ROS-dependent mechanism. Subsequent cellular consequences of oxidative stress such as DNA damage and the MAPK implication were also investigated.

Materials and methods

Materials and reagents

Unless otherwise noted, all chemicals were from Sigma.

Cell line

The human epithelial embryonic cell (EUE) line was kindly provided by Prof. Abbondandolo, Pisa, Italy. Cells were cultured in Dulbecco's Modified Eagle's medium (DMEM) supplemented with 10% fetal bovine serum (Omega Scientific inc., Tarzana, CA, USA), penicillin (100 U/ml) and streptomycin (100 µg/ml) and maintained in a humidified atmosphere containing 5% CO_2 and 95% air at 37°C. Cells were trypsinised, collected and resuspended in fresh medium twice a week.

Before treatment with AgNP, cells were exposed, where indicated, for 30 min to 2.5 µM diphenyleneiodonium (DPI), for 30 min to 2.5 mM *N*-acetyl cysteine (NAC), a ROS scavenger, or for 1 h to 10 mM U0126, an inhibitor of ERK activation.

AgNP dispersion and characterisation

Spherical AgNP of nominal diameter 20 ± 5 nm were purchased from Plasmachem GmbH, Berlin Germany. A stock solution at concentration of 2 mg/ml was prepared fresh before use in filtered distilled water, vortexed and sonicated (Labsonic®P, Sartorius Stedim Biotech, Göttingen, Germany) for 3 min (100% cycle, 100 W) on ice. After sonication, phosphate-buffered saline (PBS) and bovine serum albumin (BSA) at a final concentration of 1.5% were quickly added. Different concentrations were prepared in complete DMEM and added to the cells for the time indicated at 37°C in a 5% CO_2 atmosphere. Detailed characterisation by dynamic light scattering (DLS), scanning (SEM) and transmission (TEM) electron microscopy has already been published (9, 16). DLS measurements in DMEM immediately after dispersion detected three populations of particles; single particles (mean diameter of 33.9 nm) and medium and large agglomerates with mean diameter of 225.9 and 4050 nm, respectively. The DLS values in DMEM measured after incubation for 30 min showed only a slight shift with time. The *z*-potential of the AgNP analyzed in water at 100 µg/ml was −37.4 ± 2.5 mV (without BSA and PBS supplement) and −26.7 ± 0.8 mV (with BSA and PBS supplement). SEM analysis showed AgNP forming small agglomerates with average size of ~100 nm and a TEM image showing AgNP ranging in size between 20 and 100 nm. However, agglomerates were observed (9, 16).

ROS measurement with fluorophore dihydrodichlorofluorescein

Cells (2×10^5) were seeded in a 12-well plate 24 h prior to the exposure to AgNP for 30 min. Medium was replaced with Hank's balanced salt solution (HBSS) with no phenol red. A solution of HBSS containing 20 µM dihydrodichlorofluorescein (H_2DCF-DA) was added to the cells for 40 min. Cells were washed twice with PBS, trypsinised and collected in clean tubes. Cells were lysed using a 1% Triton solution. After centrifugation, the supernatant was used to measure in duplicate with the fluorescence at 488/515 λ excitation/emission.

Superoxide measurement

Cells (2×10^5) were seeded in a 12-well plate 24 h prior to the exposure to AgNP. Medium was replaced with HBSS with no red phenol containing 2.5 mM nitro blue tetrazolium (NBT) reagent alone or with 2.5 µM DPI for 30 min. Three different concentrations of AgNP were added to the wells for 10, 30 and 60 min followed by 5-min incubation with 7.4% formaldehyde at 37°C. Cells were then washed twice with PBS and thoroughly once with methanol. Cells were allowed to air dry and the blue formazan formed was solubilised adding 2 mM KOH and 100% dimethyl sulfoxide. The solution was collected and the optical density was measured at 630 nm.

Western blot

Proteins were resolved on 10% Tris-glycine acrylamide gel (Invitrogen, Carlsbad, CA, USA) under denaturing conditions before being transferred electrophoretically onto a polyvinylidene

difluoride membrane (Immobilon P; Millipore, Bedford, MA, USA). Membranes were blocked with 5% non-fat dry milk (NFDM) at room temperature for 1 h and then incubated overnight at 4°C with primary antibody diluted in 5% NFDM in Tris-buffered saline (TBS) as indicated (1:1000 anti-phospho p38; 1:2000 anti-phospho-ERK; 1:1000 anti-phospho-JNK; 1:2000 anti- GAPDH). After being washed with TBS containing 0.05% Tween 20, the membrane was incubated with goat anti-rabbit conjugated to horseradish peroxidase (1:2000) at room temperature for 2 h. The blots were developed by the enhanced chemiluminescence technique (ECL Plus; Amersham, Arlington Heights, IL, USA) according to the manufacturer's instructions. The bands of interest were imaged with and quantified by photon counting using the charged-coupled device camera of a Kodak Image Station 2000MM (Kodak, Rochester, NY, USA) and Kodak 1D 3.6 Image Analysis Software. Photon counting was used for graphing and statistical analysis.

DNA damage measurement with the Comet assay

The alkaline version of the comet procedure was followed according to Collins *et al*. with slight modifications (17). Pre-treated and treated cells were suspended in 1% low melting point agarose in PBS buffer (Ca^{2+} and Mg^{2+} free). A volume of 60 µl of cell suspension (~2×10^4 cells) was spread on pre-coated slides and covered with a cover slip. Cells exposed to hydrogen peroxide (250 µM, 5 min, on ice) or to the photosensitizer Ro19-8022 (kindly obtained from Hoffmann La Roche) plus visible light (1 µM in PBS, 500-W tungsten-halogen source at 30 cm, for 5 min, on ice) were used as positive controls. Slides (two for each sample) were placed in lysis solution (2.5 M NaCl, 100 mM Na_2EDTA, 10 mM Tris–HCl, pH 10 and 1% Triton X-100) for 1 h at 4°C. After lysis, half of the slides were incubated with hOGG1 enzyme (50 µl per gel, 30 min, 37°C humidified atmosphere), and then the unwinding was performed in buffer (300 mM NaOH, 1 mM Na_2EDTA, pH > 13) in an electrophoresis tank for 20 min at 4°C. A field of 25 V (0.8 V/cm, ~300 mA) was then applied for 30 min. The slides were washed in PBS (10 min) and double distilled H_2O (10 min) at 4°C. Samples were stained with 20 µl SYBR gold (0.1 µl/ml in Tris-EDTA buffer: 10 mM Tris–HCl, 1 mM EDTA, pH 7.5–8) and 100 comets (50 per gel) for each sample were scored by computerised image analysis (Comet Assay IV 4.2, Perceptive Instruments Ltd) for determination of relative tail intensity.

Statistical analysis

All data are expressed as the mean of at least three independent experiments ± SD. Analysis of variance and the Tukey's test were performed to compare the variants between experimental groups. Statistical significance was accepted when $P < 0.05$.

Results

AgNP induce production of intracellular ROS and NOX-dependent superoxide

ROS production following exposure of diverse NP, such as nanocopper, silica and iron NP, has been reported in several studies (18–20). In order to test whether oxidative stress occurred in our experimental system, we used as detection probe, H_2DCF-DA. To assess the effect of AgNP on ROS formation, EUE cells were incubated with different concentrations of AgNP for 30 min. As shown in Figure 1, AgNP induced ROS production even at the lowest concentration (1 µg/ml), as observed by H_2DCF-DA fluorescence compared with control cells. Samples treated with H_2O_2 were used as positive control. The DCF method is based on the conversion of 2′,7′ dichlorofluorescin into fluorescent 2′,7′ dichlorofluorescein by ROS, primarily peroxyl radicals and peroxides such as peroxynitrites (21–23), but it does not provide any further information on which specific ROS are produced. We also measured superoxide ($O_2^{\bullet-}$) anions produced by the cells using the NBT assay. As shown in Figure 2A, the $O_2^{\bullet-}$ production started to increase after 10 min of AgNP exposure reaching the maximum at 30 min and then decreasing to the control level after 1 h. Interestingly, our results indicate that AgNP does not induce a concentration-dependent response in EUE cells. NBT is a cell-permeable compound which has been widely used for the detection of $O_2^{\bullet-}$ anions in cells (24–26). Results in Figure 2B show that incubation with an inhibitor of the NOX family, DPI, prior to AgNP exposure for 30 min, could significantly inhibit $O_2^{\bullet-}$ formation, suggesting that most of the $O_2^{\bullet-}$ production was a consequence of enzymatic activation. We cannot, however, formally exclude a diaphorase activity (i.e. NBT would receive electrons directly from cell enzymes without a $O_2^{\bullet-}$ intermediate) (27).

AgNP induce ROS-dependent ERK and JNK phosphorylation but not p38 phosphorylation

MAPK pathways regulate several of the important biological processes in the cell such as mitosis, metabolism, survival, apoptosis and differentiation. The most extensively studied groups of MAPK to date are ERK1/2, JNK1/2 and p38 kinases. We examined the activation of ERKs, JNKs and p38 upon short-term and long-term AgNP exposure. Total extract from EUE cells treated with different concentration of AgNP for several lengths of exposure were subjected to western blot analysis using a monoclonal antibody to the phosphorylated form of ERK1/2, JNK1/2 and p38. As shown in Figure 3A, AgNP induced phosphorylation of ERK1/2 and JNK1/2 but not p38 after 30 min with a concentration-dependent increase from 1 to 25 µg/ml. The level of phosphorylation decreased to almost the control level after 1 h. Reprobing the same membrane with an anti-GAPDH antibody indicated similar protein loading in each lane. The activation of ERK1/2 and JNK1/2 was only an early response to particles treatment. This is further confirmed by results presented in Figure 3B, where 24-h treatment to AgNP did not induce phosphorylation of ERK and JNK. Interestingly, these data show that there was a correlation between the time point at which the $O_2^{\bullet-}$ formation reached the maximum and the phosphorylation of ERK and JNK.

We further examined the role of ROS in ERK and JNK activation. Western blot analysis showed that incubation of DPI and NAC prior to AgNP exposure was able to inhibit JNK and ERK phosphorylation induced by AgNP (Figure 4). This suggests that the phosphorylation/activation of both kinases is mediated by a ROS-dependent mechanism.

AgNP induce DNA oxidation damage

Although in different cell lines, cytotoxicity data concerning this AgNP dispersion have been published from our laboratory and from Lankoff *et al*. Using several cytotoxicity and viability assays, 30 min treatment with AgNP did not show any toxicity to any concentration used (1, 50, 100 µg/ml) by trypan blue exclusion or colony forming ability assays, whereas only 100 µg/ml showed cytotoxicity by relative growth activity (9). Furthermore, Lankoff *et al*. showed that also at 24-h AgNP did not induce cytotoxicity if not at higher concentrations (50, 100 µg/ml) (16). As this AgNP dispersion did not show high cytotoxicity, we next investigated its potential genotoxicity.

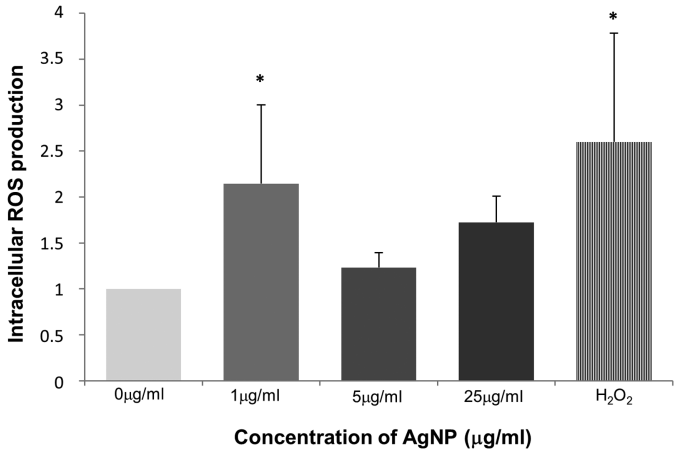

Figure 1. AgNP induced production of intracellular ROS in EUE cells. EUE cells were incubated for 40 min with 20 μM H_2DCF-DA before treatment with indicated concentration of AgNP for 30 min. Fluorescence of dichlorofluorescein (DCF) was detected by using an ex λ 488 nm and em λ 510 nm. 1 mM H_2O_2 was used as positive control. *$P < 0.05$ treatment versus control.

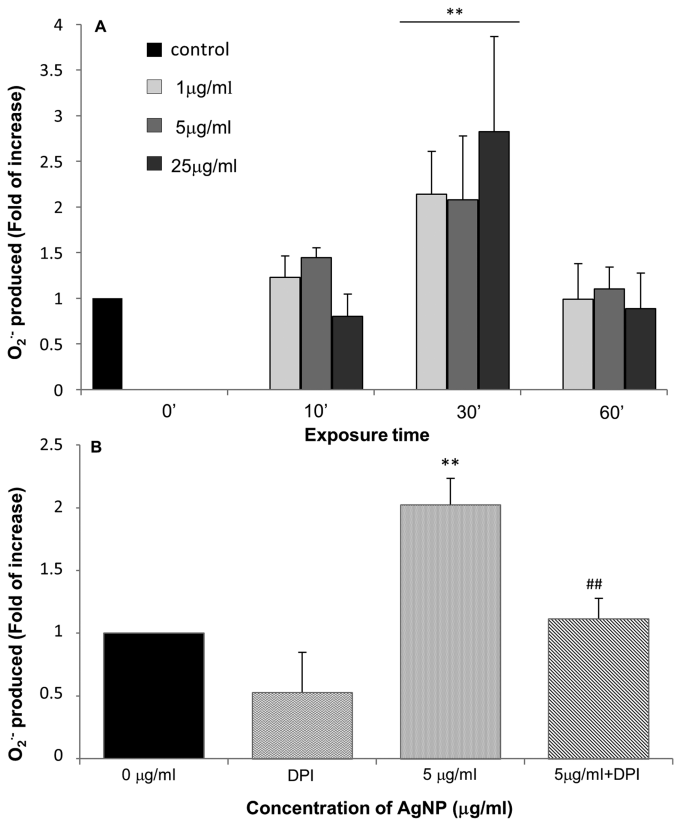

Figure 2. AgNP induced production of $O_2^{\bullet-}$. (**A**) EUE cells were incubated for 30 min with 2.5 mM NBT before treatment with different concentrations of AgNP. $O_2^{\bullet-}$ production was determined as described in Materials and methods. (**B**) Effect of 2.5 μM DPI pre-treatment on $O_2^{\bullet-}$ production. Results are expressed as fold-increase. **$P < 0.005$ treatment versus control. ##$P < 0.005$ treatment versus inhibitors.

In order to test whether AgNP induced DNA oxidation lesions, we performed the modified Comet assay using hOgg1, a glycosylase used for the detection of 8-oxoG. As observed in Figure 5A, AgNP induced a dose response of DNA oxidation lesions after 30 min of exposure in EUE cells. In contrast, no significant strand breaks were detected upon 2-h treatment. As the time frame in which the oxidative lesions were present correlated well with the $O_2^{\bullet-}$ production (Figure 2A), we next investigated whether $O_2^{\bullet-}$ played a role in the DNA oxidation. Incubation with DPI followed by AgNP exposure completely inhibited the oxidative DNA modifications measured by the comet assay, suggesting that DNA oxidation is dependent on AgNP-induced $O_2^{\bullet-}$ formation. Furthermore, DNA modifications were lower after 2-h AgNP exposure (Figure 5B), indicating that DNA repair was already induced. However, it is difficult to interpret the repair kinetics when the damaging agent is still present.

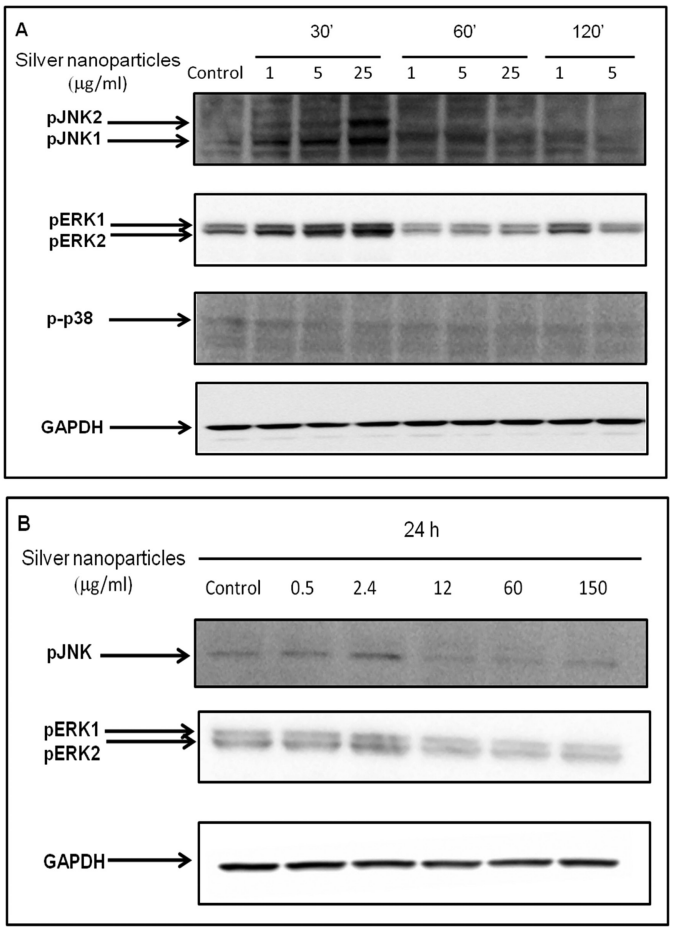

Figure 3. AgNP-induced phosphorylation/activation MAPK. EUE cells, near confluence, were treated with different concentration of NP for the indicated time, and JNK, ERK and p38 phosphorylation levels were determined by western blot with the appropriate antibody (**A** and **B**).

ERK is involved in the regulation of repair of DNA oxidation damage induced by AgNP

Increased activation of ERK, as detected by increased ERK tyrosine phosphorylation, was seen in EUE cells after 30 min of AgNP exposure (Figure 3A). Furthermore, 2 h after AgNP exposure, DNA repair was induced. To answer the question whether protection against oxidative damage to DNA was being conferred by ERK activation, the cells were plated in the presence of 10 μM U0126, an inhibitor of the ERK-activating mitogen-activating kinase (MEK). Culture for 1 h with U0126 abolished the capacity of the cells to repair DNA after 2-h exposure (Figure 5B), suggesting that protection against oxygen-induced DNA modifications by AgNP, occurred through an ERK activation-dependent pathway.

Discussion and conclusions

Even though, AgNP are among the most commercialised nanomaterials, the mechanisms that regulate AgNP toxicity are still not fully understood. The present work supports the key role of ROS in AgNP-induced genotoxicity and extends our knowledge of the AgNP-mediated mechanism of ROS generation. Finally, ERK activation seems to be involved in the regulation of repair of AgNP-induced DNA oxidation damage.

Like airborne ultrafine particles, ROS and the associated oxidative stress are proposed as a crucial mediator for NP toxicity (11, 28). However, how the presence of NP could increase the ROS formation is not completely understood. The natural property for many NP to bind transition metals is believed to enhance ROS-induced toxicity. Furthermore, the surface chemistry of particles can lead to direct ROS formation (29, 30). Additionally, NP can directly interfere with the mitochondria or enzymes producing ROS, such as NOX. Evidence that NOX2 is involved in ROS generation was shown by Mo *et al.* in a mouse pulmonary endothelium model following exposure to ultrafine particles (12). Similar evidence was suggested by the data presented here where the source of $O_2^{\bullet-}$ appeared to be due to activation of one or more NOX isoforms, as exposure to DPI, a non-specific but widely used inhibitor of NOX family, reduced the release of AgNP-induced ROS from the cell (Figure 2B).

The activity of NOX2 is regulated mainly by phosphorylation of the serines of p47 (PHOX), one of its cytosolic subunits. It is also regulated by modification of four cysteines of the same subunit, as indicated by the replacement of those cysteines by alanines (31). Given the reported ability of AgNP to influence protein structure and function following adsorption via anionic amino acids such as cysteine, one can speculate that AgNP might modulate the activity of these families of enzymes through this mechanism (32).

We next examined the role of AgNP-generated ROS, as mediator of activation of MAPK pathways, focusing on the three best-defined subgroups: p38, ERK and JNK.

It is now well accepted that ROS can induce and mediate the activation of MAPK pathways in responses to several stimuli, regulating several cell processes such as proliferation and apoptosis

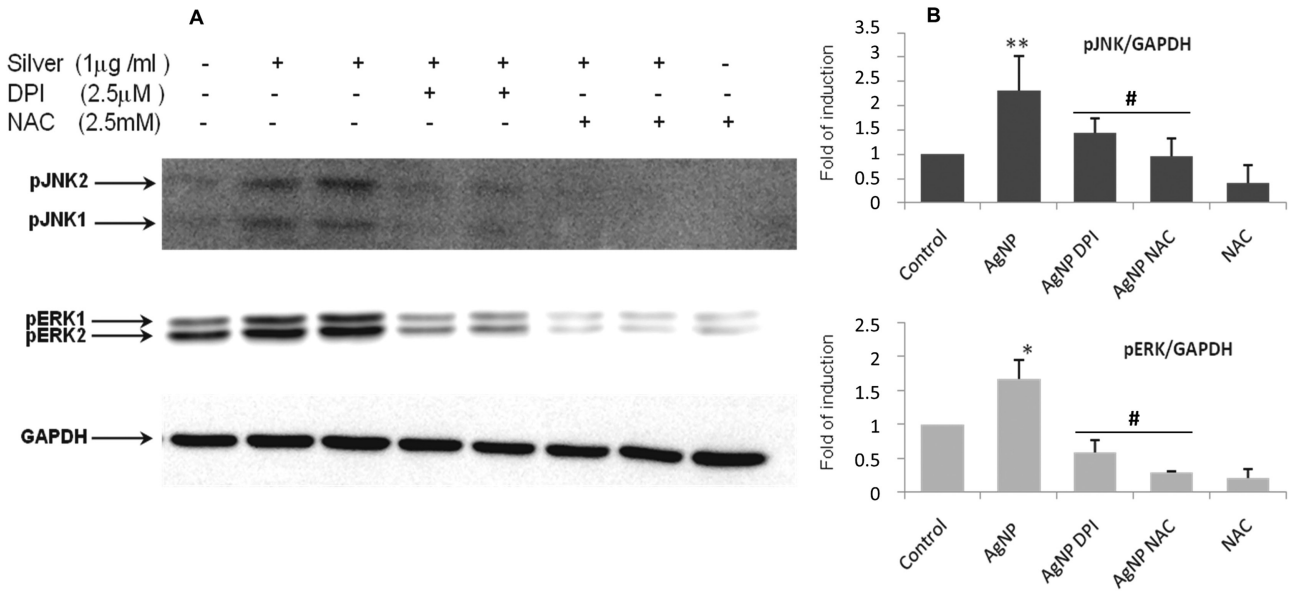

Figure 4. ROS-dependent phosphorylation/activation of JNK and ERK by AgNP exposure. EUE cells were incubated with DPI and NAC and then AgNP for 30 min. JNK and ERK phosphorylation levels were determined by western blot (**A**). The bands of interest were imaged and photon counting was quantified by using a Kodak Image Station 2000R and Kodak 1D 3.6 Image Analysis Software. Photon counting was used for creating the bar graphs (**B**). $^{**}P < 0.005$, $^{*}P < 0.05$ treatment versus control. $^{\#}P < 0.005$ treatment versus inhibitors.

(33). However, it is not clear whether ROS act as mediator of the biological effects of AgNP through the activation of MAPK or its direct involvement in cell damage, or both. Furthermore, ROS might be a direct consequence of cell mechanical injury and these mechanisms might work in concert resulting in different degrees of toxicity depending on the nature of the NP. Recently, Hsin *et al*. (2008) showed that AgNP acted through ROS and JNK to induce apoptosis (34). In contrast, Asharani *et al*. (2009) showed the direct involvement of AgNP in the disruption of mitochondrial activity and apoptosis (35). Additionally, Eom and Choi suggested that DNA damage and apoptosis were attributed to the upstream signalling mechanism of p38 MAPK (15). In contrast with the data of Eom and Choi, our results suggested that ROS produced by NOX ($O_2^{\bullet-}$ and H_2O_2 following $O_2^{\bullet-}$ dismutation) are involved in the activation of ERK and JNK but not p38, and that ROS induced oxidative DNA damage directly and not through the activation of MAPK pathways. The response of cells to AgNP in our experimental model occurred as an early event. The greatest ROS production, in fact, was reached after 30 min, the same time as the activation of ERK and JNK in the cells reached the highest level, as well as oxidative damage to the DNA. Such an early response to NP has been reported by Diaz *et al*. in Jurkat cells, where ROS production increased after short incubation times (5–30 min), whereas no ROS production was reported with longer periods of incubation (36). A variation in the time rate response to NP may be found depending on different susceptibility of cells which in turn depends on the type of NP (37).

The kinetics of cellular binding and uptake of AgNP, used in our experimental model, has been previously reported in A549, HepG2 and THP-1 cells by Lankoff *et al*. Based on the analysis of side scatter distribution ratio as measure of cellular uptake, the presence of AgNP was found in cytoplasm and organelles after 2-h exposure. However, the possibility that AgNP uptake occurs even faster cannot be ruled out as 2 h was the shortest time point of their measurement (16). Additionally, we found that AgNP were taken up by HEK 293 cells after 30-min exposure mostly as single particles in vacuoles and cytoplasm (9). Furthermore, NP uptake after 30 min has been shown in human aortic endothelial cells (HAEC) using TEM (38).

Oxidative stress has been indicated as one of the main mechanisms by which AgNP exert their toxic effect (39). It has been reported that ROS can generate a variety of DNA modifications including strand breaks, sites of base loss and oxidised purine and pyrimidine modifications (40–42). 8-Oxoguanine (8-oxoG) is one of the major base lesions formed after oxidative reaction with DNA and is responsible for the high rate of spontaneous mutations in all aerobic cells. We further examined the DNA damage induced by AgNP and the upstream signalling mechanisms responsible for the DNA oxidation lesions. Our results showed that AgNP induced mainly oxidative lesions as only the modified version of the Comet assay, using hOGG1 enzyme, could detect DNA damage. TEM experiments showed evidence of AgNP translocation into the cell nucleus (9). AgNP can, then, interact with the DNA causing genotoxicity. However, our data indicate that rather than being a consequence of direct interaction between AgNP and DNA, oxidative lesions result from ROS generated by NOX ($O_2^{\bullet-}$ and/or H_2O_2), as the AgNP toxicity could be prevented by incubation with NOX inhibitor. As ROS are short-lived species, due to the cellular antioxidant defence, it is unlikely that the ROS produced by NOX2 or any other cytosolic NOX could cause damage to DNA. One likely candidate of NOX family is NOX4. It has been previously reported that NOX4 is localised such that it delivers H_2O_2 to the nuclear compartment which causes oxidative modification of DNA (43); thus, activation of the different NOX isoforms by AgNP might depend on its cellular localisation which in turn would causes differential cell damage.

As previously mentioned, we found that DNA damage is not mediated by MAPK pathways. However, ERK pathways were found to be crucial in the process of DNA repair of oxidative damage. Our results showed that after 2 h of AgNP exposure, the DNA is completely repaired; nevertheless, the inhibition of

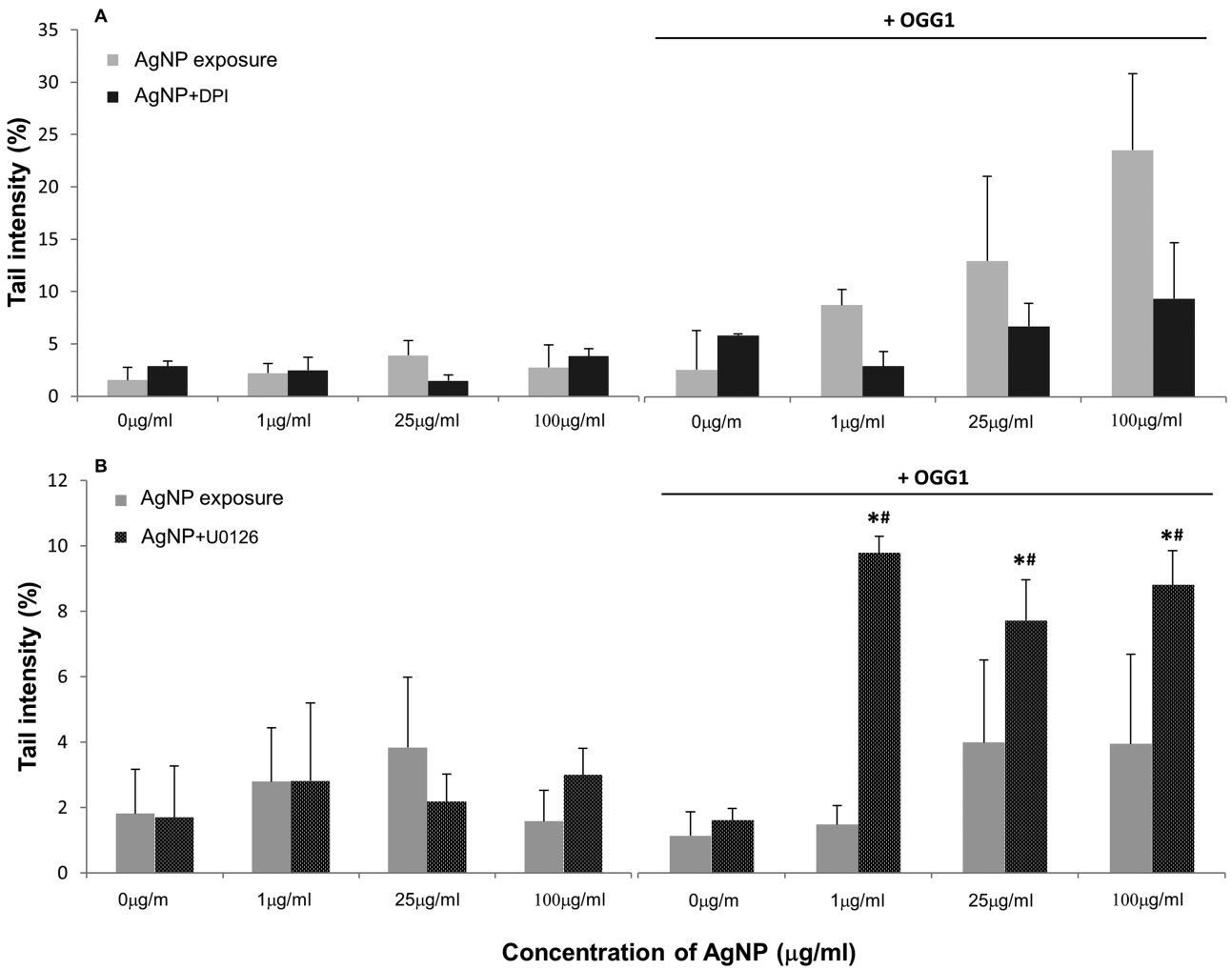

Figure 5. DNA oxidation lesions induced by AgNP and role of ERK in the repair mechanism. EUE cells were incubated either with 2.5 µM DPI (**A**) or 10 µM of U0126 (**B**) followed by treatment with AgNP for 30 min (A) or 2 h (B). DNA fluorescence was calculated to determine the extent of DNA damage by the Comet assay IV imaging software. Results are expressed in percentage of tail migration.*$P < 0.005$ treatment versus control. #$P < 0.005$ treatment versus inhibitors.

MEK, the protein directly upstream of ERK, abolished the cellular capacity for DNA repair. In accordance with our data, previous observations showed the contribution of the MEK-ERK kinases to the DNA damage response; nonetheless, the underlying mechanism remains still to be determined (44). One mechanism proposed is that ERK kinases facilitate ATM and Rad3-related protein kinase (ATR) and ataxia telangiectasia-mutated protein kinase (ATM) activation either by direct phosphorylation or through phosphorylation of other components involved in the ATR/ATM activation pathway. Additionally, because of the rapidity of the response to AgNP, another possible mechanism is that an ERK signal pathway induced by oxidative stress (AgNP mediated) might cause transfer of repair enzymes to the nucleus, their site of action (45).

Taken together, these data show that AgNP genotoxicity is mainly mediated by ROS production and that a ROS-engaged ERK pathway is critical for the cytoprotection against AgNP toxicity.

Funding

This work was supported by an European Economic Area (EEA) Polish-Norwegian research grant (PNRF-122-AI-1/07); FP7-PEOPLE-IEF Marie Curie grant (PIEF-GA-252858).

Conflict of interest statement:

None declared.

References

1. Limbach, L. K., Li, Y., Grass, R. N., Brunner, T. J., Hintermann, M. A., Muller, M., Gunther, D. and Stark, W. J. (2005) Oxide nanoparticle uptake in human lung fibroblasts: effects of particle size, agglomeration, and diffusion at low concentrations. *Environ. Sci. Technol.*, 39, 9370–9376.
2. Limbach, L. K., Wick, P., Manser, P., Grass, R. N., Bruinink, A. and Stark, W. J. (2007) Exposure of engineered nanoparticles to human lung epithelial cells: influence of chemical composition and catalytic activity on oxidative stress. *Environ. Sci. Technol.*, 41, 4158–4163.
3. Jiang, X., Miclaus, T., Wang, L., Foldbjerg, R., Sutherland, D. S., Autrup, H., Chen, C., and Beer, C. (2014) Fast intracellular dissolution and persistent cellular uptake of silver nanoparticles in CHO-K1 cells: implication for cytotoxicity. *Nanotoxicology*. 2014 April 16 [Epub ahead of print]. doi:10.3109/17435390.2014.907457
4. Kruszewski, M., Brzoska, K., Brunborg, G. *et al.* (2011) Toxicity of silver nanomaterials in higher eukaryotes. In Fishbein, J. C. (ed.), *Advances in Molecular Toxicology*. Vol. 5. Elsevier, Baltimore, MD, pp. 179–218.
5. Doak, S. H., Griffiths, S. M., Manshian, B., Singh, N., Williams, P. M., Brown, A. P. and Jenkins, G. J. (2009) Confounding experimental considerations in nanogenotoxicology. *Mutagenesis*, 24, 285–293.

6. Ahamed, M., Alsalhi, M. S. and Siddiqui, M. K. (2010) Silver nanoparticle applications and human health. *Clin. Chim. Acta*., 411, 1841–1848.
7. Ahamed, M., Karns, M., Goodson, M., Rowe, J., Hussain, S. M., Schlager, J. J. and Hong, Y. (2008) DNA damage response to different surface chemistry of silver nanoparticles in mammalian cells. *Toxicol. Appl. Pharmacol*., 233, 404–410.
8. Foldbjerg, R., Dang, D. A. and Autrup, H. (2011) Cytotoxicity and genotoxicity of silver nanoparticles in the human lung cancer cell line, A549. *Arch. Toxicol*., 85, 743–750.
9. Hudecová, A., Kusznierewicz, B., Rundén-Pran, E. *et al.* (2012) Silver nanoparticles induce premutagenic DNA oxidation that can be prevented by phytochemicals from *Gentiana asclepiadea*. *Mutagenesis*, 27, 759–769.
10. Kim, S., Choi, J. E., Choi, J., Chung, K. H., Park, K., Yi, J. and Ryu, D. Y. (2009) Oxidative stress-dependent toxicity of silver nanoparticles in human hepatoma cells. *Toxicol. In Vitro*, 23, 1076–1084.
11. Nel, A., Xia, T., Mädler, L. and Li, N. (2006) Toxic potential of materials at the nanolevel. *Science*, 311, 622–627.
12. Mo, Y., Wan, R., Chien, S., Tollerud, D. J. and Zhang, Q. (2009) Activation of endothelial cells after exposure to ambient ultrafine particles: the role of NADPH oxidase. *Toxicol. Appl. Pharmacol*., 236, 183–193.
13. Carlson, C., Hussain, S. M., Schrand, A. M., Braydich-Stolle, L. K., Hess, K. L., Jones, R. L. and Schlager, J. J. (2008) Unique cellular interaction of silver nanoparticles: size-dependent generation of reactive oxygen species. *J. Phys. Chem. B*, 112, 13608–13619.
14. Hussain, S. M., Hess, K. L., Gearhart, J. M., Geiss, K. T. and Schlager, J. J. (2005) *In vitro* toxicity of nanoparticles in BRL 3A rat liver cells. *Toxicol. In Vitro*, 19, 975–983.
15. Eom, H. J. and Choi, J. (2010) p38 MAPK activation, DNA damage, cell cycle arrest and apoptosis as mechanisms of toxicity of silver nanoparticles in Jurkat T cells. *Environ. Sci. Technol*., 44, 8337–8342.
16. Lankoff, A., Sandberg, W. J., Wegierek-Ciuk, A. *et al.* (2012) The effect of agglomeration state of silver and titanium dioxide nanoparticles on cellular response of HepG2, A549 and THP-1 cells. *Toxicol. Lett*., 208, 197–213.
17. Collins, A. R. and Dusinská, M. (2002) Oxidation of cellular DNA measured with the comet assay. *Methods Mol. Biol*., 186, 147–159.
18. Khan, M. I., Mohammad, A., Patil, G., Naqvi, S. A., Chauhan, L. K. and Ahmad, I. (2012) Induction of ROS, mitochondrial damage and autophagy in lung epithelial cancer cells by iron oxide nanoparticles. *Biomaterials*, 33, 1477–1488.
19. Passagne, I., Morille, M., Rousset, M., Pujalté, I. and L'azou, B. (2012) Implication of oxidative stress in size-dependent toxicity of silica nanoparticles in kidney cells. *Toxicology*, 299, 112–124.
20. Sarkar, A., Das, J., Manna, P. and Sil, P. C. (2011) Nano-copper induces oxidative stress and apoptosis in kidney via both extrinsic and intrinsic pathways. *Toxicology*, 290, 208–217.
21. Halliwell, B. and Whiteman, M. (2004) Measuring reactive species and oxidative damage *in vivo* and in cell culture: how should you do it and what do the results mean? *Br. J. Pharmacol*., 142, 231–255.
22. Myhre, O., Andersen, J. M., Aarnes, H. and Fonnum, F. (2003) Evaluation of the probes 2',7'-dichlorofluorescin diacetate, luminol, and lucigenin as indicators of reactive species formation. *Biochem. Pharmacol*., 65, 1575–1582.
23. Possel, H., Noack, H., Augustin, W., Keilhoff, G. and Wolf, G. (1997) 2,7-Dihydrodichlorofluorescein diacetate as a fluorescent marker for peroxynitrite formation. *FEBS Lett*., 416, 175–178.
24. Berridge, M. V., Herst, P. M. and Tan, A. S. (2005) Tetrazolium dyes as tools in cell biology: new insights into their cellular reduction. *Biotechnol. Annu. Rev*., 11, 127–152.
25. Patterson, C., Ruef, J., Madamanchi, N. R. *et al.* (1999) Stimulation of a vascular smooth muscle cell NAD(P)H oxidase by thrombin. Evidence that p47(phox) may participate in forming this oxidase *in vitro* and *in vivo*. *J. Biol. Chem*., 274, 19814–19822.
26. Serrander, L., Cartier, L., Bedard, K. *et al.* (2007) NOX4 activity is determined by mRNA levels and reveals a unique pattern of ROS generation. *Biochem. J*., 406, 105–114.
27. Auclair, C., Torres, M. and Hakim, J. (1978) Superoxide anion involvement in NBT reduction catalyzed by NADPH-cytochrome P-450 reductase: a pitfall. *FEBS Lett*., 89, 26–28.
28. Li, N., Sioutas, C., Cho, A. *et al.* (2003) Ultrafine particulate pollutants induce oxidative stress and mitochondrial damage. *Environ. Health Perspect*., 111, 455–460.
29. Nel, A. (2005) Atmosphere. Air pollution-related illness: effects of particles. *Science*, 308, 804–806.
30. Oberdörster, G., Maynard, A., Donaldson, K. *et al.*; ILSI Research Foundation/Risk Science Institute Nanomaterial Toxicity Screening Working Group. (2005) Principles for characterizing the potential human health effects from exposure to nanomaterials: elements of a screening strategy. *Part. Fibre Toxicol*., 2, 8.
31. Babior, B. M. (2002) The leukocyte NADPH oxidase. *Isr. Med. Assoc. J*., 4, 1023–1024.
32. Pakiari, A. H. and Jamshidi, Z. (2007) Interaction of amino acids with gold and silver clusters. *J. Phys. Chem. A*, 111, 4391–4396.
33. McCubrey, J. A., Lahair, M. M. and Franklin, R. A. (2006) Reactive oxygen species-induced activation of the MAP kinase signaling pathways. *Antioxid. Redox Signal*., 8, 1775–1789.
34. Hsin, Y. H., Chen, C. F., Huang, S., Shih, T. S., Lai, P. S. and Chueh, P. J. (2008) The apoptotic effect of nanosilver is mediated by a ROS- and JNK-dependent mechanism involving the mitochondrial pathway in NIH3T3 cells. *Toxicol. Lett*., 179, 130–139.
35. AshaRani, P. V., Low Kah Mun, G., Hande, M. P. and Valiyaveettil, S. (2009) Cytotoxicity and genotoxicity of silver nanoparticles in human cells. *ACS Nano*, 3, 279–290.
36. Díaz, B., Sánchez-Espinel, C., Arruebo, M. *et al.* (2008) Assessing methods for blood cell cytotoxic responses to inorganic nanoparticles and nanoparticle aggregates. *Small*, 4, 2025–2034.
37. Albanese, A., Tang, P. S. and Chan, W. C. (2012) The effect of nanoparticle size, shape, and surface chemistry on biological systems. *Annu. Rev. Biomed. Eng*., 14, 1–16.
38. Kennedy, I. M., Wilson, D., Barakat, A. I., and Committee, H. E. I. H. R. (2009) Uptake and inflammatory effects of nanoparticles in a human vascular endothelial cell line. *Research Report*, *Health Eff Inst*, 136, 3–32.
39. Schrand, A. M., Dai, L., Schlager, J. J. and Hussain, S. M. (2012) Toxicity testing of nanomaterials. *Adv. Exp. Med. Biol*., 745, 58–75.
40. Cadet, J., Douki, T. and Ravanat, J. L. (2011) Measurement of oxidatively generated base damage in cellular DNA. *Mutat. Res*., 711, 3–12.
41. Kryston, T. B., Georgiev, A. B., Pissis, P. and Georgakilas, A. G. (2011) Role of oxidative stress and DNA damage in human carcinogenesis. *Mutat. Res*., 711, 193–201.
42. Shi, S., Hudson, F. N., Botta, D., McGrath, M. B., White, C. C., Neff-LaFord, H. D., Dabrowski, M. J., Singh, N. P. and Kavanagh, T. J. (2007) Over expression of glutamate cysteine ligase increases cellular resistance to H2O2-induced DNA single-strand breaks. *Cytometry. A*, 71, 686–692.
43. Gordillo, G., Fang, H., Park, H. and Roy, S. (2010) Nox-4-dependent nuclear H2O2 drives DNA oxidation resulting in 8-OHdG as urinary biomarker and hemangioendothelioma formation. *Antioxid. Redox Signal*., 12, 933–943.
44. Wei, F., Yan, J. and Tang, D. (2011) Extracellular signal-regulated kinases modulate DNA damage response - a contributing factor to using MEK inhibitors in cancer therapy. *Curr. Med. Chem*., 18, 5476–5482.
45. Mitra, S., Izumi, T., Boldogh, I., Bhakat, K. K., Chattopadhyay, R. and Szczesny, B. (2007) Intracellular trafficking and regulation of mammalian AP-endonuclease 1 (APE1), an essential DNA repair protein. *DNA Repair (Amst)*., 6, 461–469.